International Journal of Hydrogen Energy 202 (2026) 153107

Contents lists available at ScienceDirect

International Journal of Hydrogen Energy

journal homepage: www.elsevier.com/locate/he

Tuning membraneless microbial electrolysis cells operation alters efficiency and anodic microbiome toward scalable hydrogen production from sludge-hydrolysate

Mahshid Golalikhani [a], Christian Jonas Lapp [a], Nikhil Shylaja Prakash [b], Andrea Hille-Reichel [b,c], Johannes Gescher [a,*], Ahmed Elreedy [a,**]

[a] Institute of Technical Microbiology, Hamburg University of Technology, Hamburg, 21073, Germany
[b] DVGW-Research Center at the Engler-Bunte-Institut, Water Chemistry and Water Technology, Karlsruhe Institute of Technology, Karlsruhe, 76131, Germany
[c] Engler-Bunte-Institute Water Chemistry and Water Technology, Karlsruhe Institute of Technology, Karlsruhe, 76131, Germany

ARTICLE INFO

Keywords:
Bioelectrochemical systems
Coulombic efficiency
Anodic biofilm
Methanogens mitigation
Upscaling
Cathodic hydrogen recovery

ABSTRACT

The practical implementation of microbial electrolysis cells (MECs) is hindered by challenges in optimizing system performance with complex substrates. This study addresses that gap by evaluating MECs fed with hydrolysate, an appealing substrate rich in organic-acids. Through systematic variation of substrate concentration (20–60 %), pH (5–8), and applied anodic potential (−0.2 to +0.4 V vs standard hydrogen electrode [SHE]), the optimal operational conditions were defined as 40 %-hydrolysate, pH 8, and +0.4 V vs SHE, yielding a mean current density of 3.4 A/m^2 and coulombic efficiencies (CE) of 38 % and 96 % based on total organic carbon (TOC) and total volatile fatty acids (VFAs), respectively. Scalability was demonstrated using a 10 L rotating disk bioelectrochemical reactor (RDBER) at 0 and 0.4 V vs SHE, achieving a maximum hydrogen production rate of 30.57 L/m^2/d and minimal methane formation at 0.4 V. These findings offer a framework for optimizing MECs under real-feedstock conditions.

1. Introduction

Rising global demand for clean energy is driving a wave of innovation in renewable technologies, offering a powerful path away from fossil fuels and toward sustainable development. Among various energy carriers, hydrogen (H_2) has emerged as a particularly promising candidate, offering high energy density, clean combustion, economic viability, and broad environmental benefits. These features position it as a key solution to the challenges of rising global energy demand [1,2]. Microbial electrolysis cells (MECs) are bioelectrochemical systems in which exoelectrogenic bacteria oxidize organic matter at the anode, producing carbon dioxide (CO_2), protons (H^+), and electrons (e^-). These electrons are transferred to the cathode, where, under an externally applied voltage, they reduce protons to generate hydrogen gas [3,4]. The merit of using MECs for hydrogen production is their ability to simultaneously treat a variety of wastewaters by removing organic and inorganic pollutants [5,6]. The utilization of organic waste for energy generation aligns with several sustainable development goals (SDGs), i.e., clean water and sanitation (SDG 6), renew-able energy (SDG 7), public health protection (SDGs 3; 11), resource value (SDG 12) and climate action (SDG 13), as well as the European Union's strategy to reduce reliance on fossil fuels through biofuel production [7].

One of the major components of MECs is the proton exchange membrane (PEM), which separates the biotic anode from the abiotic cathode compartments. However, PEMs present certain limitations, such as high cost and increased internal resistance, which reduce the overall feasibility of the system. To address this, by excluding the PEM and operating under industrial conditions, substrate complexity and operational conditions become the main factors influencing system efficiency, primarily by shaping the MEC microbiome and affecting competing pathways such as methanogenesis. Combining such strategic operational controls, i.e., substrate, pH, and anodic potential, can selectively inhibit methanogens, thereby improving membraneless MEC performance by enhancing electron transfer efficiency and increasing hydrogen yield.

First, substrate composition plays a central role, as it determines the

* Corresponding author.
** Corresponding author.
E-mail addresses: johannes.gescher@tuhh.de (J. Gescher), ahmed.elreedy@tuhh.de (A. Elreedy).

https://doi.org/10.1016/j.ijhydene.2025.153107
Received 8 September 2025; Received in revised form 15 December 2025; Accepted 17 December 2025
Available online 20 December 2025
0360-3199/© 2025 The Authors. Published by Elsevier Ltd on behalf of Hydrogen Energy Publications LLC. This is an open access article under the CC BY license (http://creativecommons.org/licenses/by/4.0/).

availability of biodegradable organic matter and electron donors. High organic loading can enhance the current generation up to a certain threshold. Beyond this point, it may lead to substrate inhibition, accumulation of volatile fatty acids (VFAs), or stimulation of methanogens, effects that are particularly pronounced using complex, industrial substrates such as hydrolysates [8,9]. Methanogens are a major challenge in MECs because they compete with exoelectrogens for substrates and electrons, as both acetate and hydrogen can be diverted toward methane formation [10]. Acetoclastic methanogens compete with exoelectrogens for acetate, thereby decreasing electron transfer efficiency to the anode and corresponding cathodic hydrogen production. In addition, hydrogenotrophic methanogens are able to directly utilize hydrogen and CO_2 for methane formation, thereby lowering the cathodic hydrogen recovery [11]. By consuming hydrogen and acetate, they reduce the electrons available for hydrogen production, lowering overall efficiency. Excess substrate concentration can result in VFA accumulation, creating niches for methanogens and diverting electrons to methane production rather than electricity [12]. In addition, denitrifying and sulfate-reducing bacteria can act as alternative electron sinks in complex media, such as sludge hydrolysate, that would otherwise be transferred to the anode by exoelectrogens [13,14]. Therefore, optimizing substrate concentration is crucial for enhancing energy recovery in MECs.

Second, the pH of the process directly affects microbial metabolic activity, proton gradients across biofilms, and the efficiency of hydrogen evolution reactions at the cathode. Neutral to slightly alkaline conditions (pH 7–8) have also been shown to support optimal exoelectrogenic activity and hydrogen recovery [15,16]; however, the optimal pH can shift depending on the substrate buffering capacity, nutrient profile. It also depends on the operational goal, whether focused on maximizing hydrogen yield, enhancing chemical oxygen demand (COD) removal, or maintaining microbial community resilience. Adjusting the pH, away from 6.5 to 7.5, may suppress methanogenic activity, as methanogens generally prefer neutral conditions [17]. Third, the applied anodic potential is another critical factor in MECs, as it governs the thermodynamics and kinetics of extracellular electron transfer (EET). A more positive anodic potential can enhance electron extraction and increase current density, thereby improving hydrogen output. However, it also influences microbial community structure and may selectively enrich or inhibit specific functional groups within the biofilm [18,19]. Meanwhile, applying optimal anodic potentials can enrich electroactive bacteria at the anode, thereby reducing acetate availability for methanogens. In parallel, enhanced cathodic H_2 production increases the H_2 partial pressure, which further suppresses hydrogenotrophic methanogens. Combining such strategic operational controls, i.e., substrate, pH, and anodic potential, can selectively inhibit methanogens, thereby improving membraneless MEC performance by enhancing electron transfer efficiency and increasing hydrogen yield.

The lack of studies conducted under industrial conditions is considered a critical gap, as scale-up often introduces operational and biological challenges that can significantly reduce MECs efficiency [16–19]. While MEC optimization studies have mostly used synthetic feed (and sterile, in many cases) [20–24], selected feedstocks, such as hydrolysate from the dark fermentation process, offer high organic-acid content and broad availability but present challenges, including compositional variability, nutrient imbalances, and the presence of inhibitory compounds (e.g., ammonia, sulfides, and/or heavy metals). Widely studied exoelectrogens, such as *Geobacter* and *Shewanella*, catalyze anodic oxidation of only a limited set of short-chain fatty acids, like acetate, propionate, and lactate, raising questions about how they cooperate or compete within mixed microbial communities on diverse organic carbon sources [9], and how operational conditions influence this interaction to enhance cathodic hydrogen recovery. For instance, by using a pure culture of *G. sulfurreducens*, we could previously demonstrate the inhibiting effect of butyrate ($\geq$10 mM) as well as Na^+ ($\geq$100 mM) [25]. Moreover, real wastewater may exhibit low conductivity and insufficient alkalinity. Low ionic strength leads to higher ohmic losses, while weak buffering capacity results in pH gradients that impair anodic biofilm activity and reduce MEC efficiency [26]. Overall, such substrate complexity can compromise MEC performance and stability through its effects on microbial community dynamics in both planktonic and biofilm phases.

Therefore, advancing MECs toward real-world application requires a clear understanding of how operational parameters influence performance under real wastewater conditions. However, MEC optimization using primary sludge hydrolysate remains largely unexplored. In this study, a systematic investigation of the effects of hydrolysate concentration, pH, and applied anodic potential on the performance of membraneless MECs using real hydrolysate obtained from primary sludge fermentation. We examined the impact of substrate concentration on the balance between electron donor availability and potential inhibitory effects, assessed the influence of pH, and explored the role of anodic potential in modulating electron transfer efficiency and shaping the anodic microbial community composition. Through the integration of electrochemical measurements, carbon utilization analysis, and metagenomic profiling, this research provides a comprehensive understanding of how to mitigate potential competing pathways in membraneless MECs along with enhancing electroactive bacteria and optimizing hydrogen production was aimed. Furthermore, the optimized operational conditions identified were applied in a scaled-up MEC system to assess hydrogen production, and a techno-economic analysis was conducted to evaluate the overall feasibility of the process.

2. Materials and methods

2.1. Hydrolysate characteristics

The hydrolysate utilized in this study was derived from a semi-technical pilot-scale system located at the Büsnau wastewater treatment plant in Stuttgart, Germany (equivalent population 10,000). It was produced via dark fermentation of primary sludge, as substrate, operated under controlled conditions, including hydraulic retention time (HRT) of 36 h, pH of 7, and temperature of 32 °C, as reported in details in our partners' earlier publication [27]. Following fermentation, a two-step particle separation process was performed using a chamber filter press and subsequent microfiltration. Afterwards, the hydrolysate was centrifuged, step-filtered using a 0.45 μm filter, and stored at 4 °C until use in experiments. The detailed characteristics of hydrolysate is

Table 1
Characteristics of the fermentation hydrolysate used in this study.

Parameter	Unit	Value
Total organic carbon (TOC)	mM	350 ± 4
Total inorganic carbon (TIC)	mM	11 ± 1
Total nitrogen (TNb)	mM	37.3 ± 1.2
Total Phosphorus (TP)	mg/L	269 ± 11
Acetate	mM	34.28 ± 0.03
Propionate	mM	25.67 ± 0.35
Butyrate	mM	3.4 ± 0.3
Lactate	mM	ND
NH_4^+-N	mg/L	154 ± 4
NO_3^-	mg/L	2.58 ± 0.26
Ca^{2+}	mg/L	421 ± 71
Fe^{2+}	mg/L	1.1 ± 0.3
K^+	mg/L	60.84 ± 7.05
Mg^{2+}	mg/L	51.77 ± 4.99
Mn^{2+}	mg/L	0.92 ± 0.14
Na^+	mg/L	114 ± 9
S	mg/L	25.1 ± 3.1
Si^{4+}	mg/L	11.2 ± 3.2
Zn^{2+}	mg/L	3.01 ± 0.58
Cl^-	mg/L	164 ± 19
SO_4^{2-}	mg/L	20.85 ± 2.71
Ionic conductivity	mS/cm	8.75 ± 0.56
pH		4.2 ± 0.4

ND, not detected.

shown in Table 1.

2.2. MEC setups and experimental design

A 250 mL cylindrical microbial electrolysis cell (C-MEC), as previously described by Härrer et al. [25], was used in this study (see supplementary material). The anode, made of graphite felt (6 × 3 cm, GFD 2.5, SGL Group, Germany), provided a total projected surface area of 36 cm^2. Prior to use, it was sequentially rinsed with isopropanol and deionized water. The cathode was composed of a platinum mesh (104 mesh/cm^2, Chempur, Germany) with an active surface area of 1.25 cm^2. The Ag/AgCl reference electrode was used to set the anodic potential at 0 V versus standard hydrogen electrode (SHE), corresponding to −0.199 V vs. Ag/AgCl. Chronoamperometric measurements were carried out using a Gamry Interface 1010 single-channel potentiostat (GAMRY Instruments, USA). During operation, the MECs were maintained at 30 °C inside an incubator and continuously stirred using magnetic stirrers. Anoxic conditions were maintained throughout the experiments by purging the headspace with a gas mixture of 80 % N_2 and 20 % CO_2. The wild-type strain *Geobacter sulfurreducens* PCA was used as starting inoculum to promote the development of a stable and electroactive biofilm. The strain was pre-cultured at 30 °C for approximately 48 h in a growth medium containing 15 mM sodium acetate and 40 mM fumarate, following the protocol described by Klein et al. [28]. The suspension was then inoculated into the first C-MECs at a final OD_{600} of 0.1.

Prior to starting the series of optimization experiments, the C-MECs inoculated solely with *G. sulfurreducens* were fed with hydrolysate. Once biofilm enrichment and system stabilization were achieved, a piece of the anodic graphite felt (3 cm^2) was vortexed in fresh hydrolysate, and 1 mL of the suspension was introduced into each C-MECs used for the first series of experiments. By doing this procedure, the initial grown planktonic cells are excluded between each feed-cycle. As illustrated in Fig. 1, the experimental sequence began by evaluating the effect of hydrolysate concentration (20 %, 40 %, and 60 %) on MEC performance. After this step, the medium in the reactors was replaced with fresh hydrolysate at the concentration that showed the highest efficiency to investigate the effect of pH, tested across a range of 5, 5.5, 6, 6.5, 7, and 8. Following pH optimization, the reactors were refreshed with hydrolysate adjusted to the previously determined optimal pH to assess the impact of the applied anodic potential, which was varied at −0.2 V, 0 V, +0.2 V, and +0.4 V vs. SHE. All experiments were conducted in batch mode, performed in triplicate, and the results are presented as mean ± standard deviation.

Afterwards, to validate the obtained optimal operational conditions in a scalable design, a 10 L rotating disk bioelectrochemical reactor (RDBER) was used (see supplementary material), as also described in an earlier application [29,30]. Briefly, graphite plates (total anodic surface area of 0.5 m^2) served as the anode, and titanium-coated half-disc electrodes (0.25 m^2 total area) were used as cathodes. A reference electrode (SE23I, Sensortechnik Meinsberg, Germany) was connected externally. The complete system, including peripheral components, had a total volume of 12.6 L. Temperature was maintained using heating mats, and pH was automatically regulated via a Biostat® control unit. Fluid circulation was achieved using a peristaltic pump (Masterflex™, Fisher Scientific) connected to stainless steel piping. Anodic potential was controlled using a potentiostat (Gamry Interface 5000E). Anode rotation was maintained at 1 RPM using a stepper motor. In the first operational cycle of RDBER, *G. sulfurreducens* was inoculated at an initial OD_{600} of 0.1 in the synthetic medium used during pre-culturing, containing 15 mM acetate but excluding fumarate. Afterwards, two consecutive fed-batch cycles were employed using real hydrolysate, and by applying anodic potential of 0 V and +0.4 V, respectively (Fig. 1).

2.3. Analytical methods and calculations

The acetate, propionate, and butyrate concentrations were measured using a high-performance liquid chromatography (HPLC) system (UltiMate 3000 SD, Thermo Scientific, Waltham, MA, USA) equipped with an Aminex HPX-87H column (300 × 7.8 mm, Bio-Rad, Munich, Germany). Detection was performed using a UV detector at 275 nm, and data

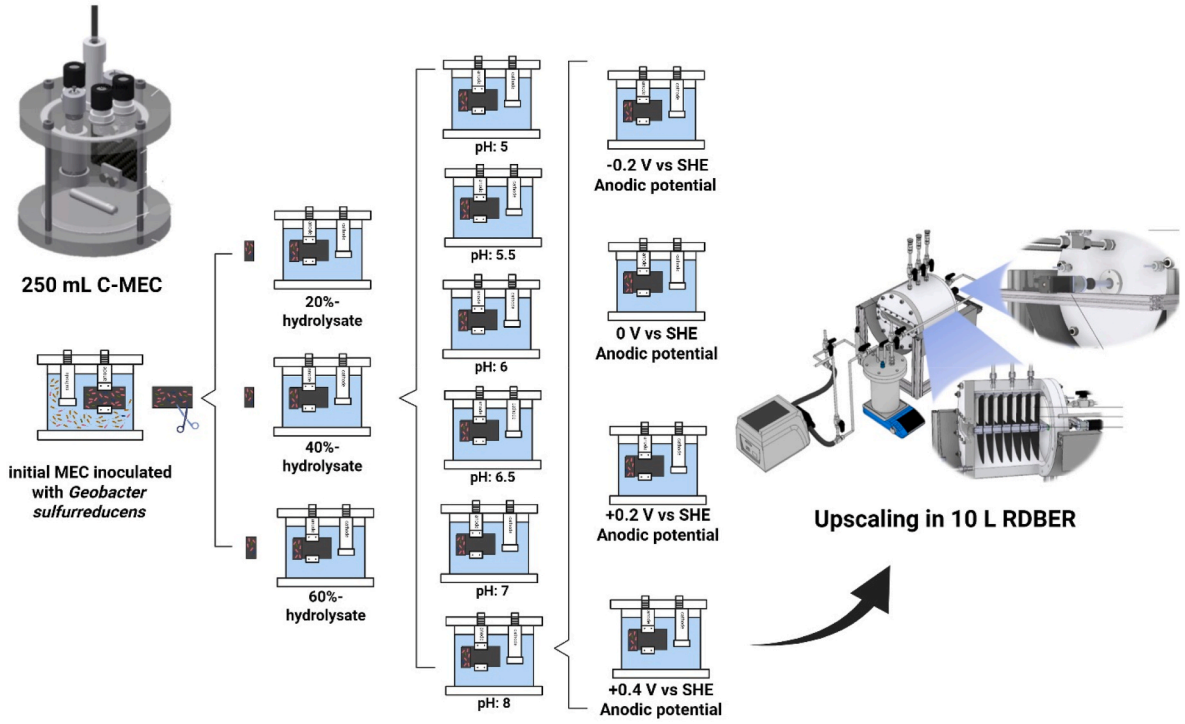

Fig. 1. Schematic of the cylindrical microbial electrolysis cell (C-MEC) setup and experimental design. The system was filled with unsterile hydrolysate and enriched with *Geobacter sulfurreducens* over 10 days. Subsequently, the carbon felt anode was distributed to fresh MECs operated under varying hydrolysate concentrations (20 %, 40 %, and 60 %), pH values (5–8), and applied anodic potentials (−0.2 to +0.4 V vs. standard hydrogen electrode (SHE)).

analysis was managed via Chromeleon 11 software. Before injection, samples were filtered through 0.2 μm PTFE membrane syringe filters. The mobile phase consisted of 5 mM sulfuric acid, delivered at a flow rate of 0.6 mL/min. The column temperature was maintained at 45 °C throughout the analysis. The total organic carbon (TOC) content in the samples was measured using a DIMATOC® 2100 analyzer (DIMATEC Analysentechnik GmbH). The major inorganic constituents in the hydrolysate were quantified using an ion chromatography (IC) system for anions, i.e., NO_3^-, SO_4^-, and Cl^-, (790 Personal; Metrohm, Switzerland), and an inductively coupled plasma optical emission spectroscopy (ICP-OES) spectrometer 5110 (Agilent, USA) was used for the rest. Gas volume was quantified using a BlueVCount gas counter (BlueSens, Herten, Germany), which enables real-time monitoring of gas flows. Gas composition was analyzed using micro-GC 490 supported with PPQ and MolSieve columns (Agilent, USA).

The mean current density was calculated using Eq. (1), with J (A/m^2) representing the current density over the anode surface area (m^2) and t (s) corresponding to the time interval. CE was calculated as shown in Eq. (2), where I is the current (A) generated overtime t (s), F is Faraday's constant (96,485 C/mol), b is the number of theoretical moles of electrons released per mole of oxidized compound (4 for TOC), and $\Delta(M)$ (moles) represents the electron donor consumption during this period.

$$\text{Mean current density} = \frac{\int_0^t J\,dt}{t} \tag{1}$$

$$\text{CE}\ (\%) = \frac{\int_0^t I\,dt}{F \cdot b \cdot \Delta(M)} \tag{2}$$

Hydrogen energy efficiency (η_{H2}) was determined by quantifying the energy content of hydrogen produced relative to the electrical energy input, using Eq. 3; n_{H2} represents the moles of hydrogen generated, and ΔH_{H2} is the calorific value difference of hydrogen in comparison to electrical energy of 285.83 kJ/mol. The electrical energy input (E_{input}, in kJ) was computed by integrating the product of voltage (V) and current (A) measured over the experimental period. Cathodic hydrogen recovery efficiency ($\eta_{cat,H2}$) was calculated to evaluate the efficiency of hydrogen production at the cathode relative to the electrical current supplied. It was determined by dividing the experimentally measured moles of hydrogen ($n_{H2,measured}$) by the theoretical moles of hydrogen ($n_{H2,theoretical}$), calculated using Faraday's law based on the total charge transferred. The calculation is presented in Eq. 4, and theoretical hydrogen production is defined in Eq. 5. To assess energy efficiency, hydrogen yield per unit of energy input (kg H_2/kWh) was calculated (Eq. 6), m_{H2} is the mass of hydrogen produced (kg/day m^2), and E_{input} is the electrical energy input (kWh/day m^2). The H_2 production cost (€/kg H_2) quantifies the energy-related expense associated with producing 1 kg of hydrogen, calculated using the system's electrical energy input and the unit electricity price, as shown in Eq. 7, using current electricity price of 0.18 €/kWh [31]; E_{input} is electrical energy input (kWh), C_{elec} is unit cost of electricity (€/kWh) and m_{H2} is theoretical mass of hydrogen produced (kg). The net economic yield of hydrogen (€/kg H_2) represents the financial return per kilogram of hydrogen generated. It is calculated as the difference between the average market selling price of hydrogen (10 €/kg) and its production cost [32]. In this study, only the cost of electrical energy input was taken into account (Eq. 8).

$$\eta_{H_2} = \frac{n_{H_2} \cdot \Delta H_{H_2}}{E_{input}} \tag{3}$$

$$\eta_{cat,H_2} = \frac{n_{H_2,measured}}{n_{H_2,theoretical}} \tag{4}$$

$$\text{Theoretical } H_2 \text{ production} = \frac{I \int dt}{2F} \tag{5}$$

$$Y_{H_2/E} = \frac{E_{H_2}}{E_{input}} \times 100 \tag{6}$$

$$H_2 \text{ production cost} = \frac{E_{input} \times C_{elec}}{m_{H_2}} \tag{7}$$

$$H_2 \text{ net economic yield} = H_2 \text{ market price} - H_2 \text{ production cost} \tag{8}$$

2.4. Microbial community identification

To examine microbial community composition, whole genome sequencing was performed Nanopore sequencing (Oxford Nanopore Technologies, Oxford, UK); it was carried out using a MinION Mk1b device fitted with a R10.4.1 flow cell and run with MinKNOW software version 22.10.7. For this purpose, 3 cm^2 pieces of anodic graphite felt were collected under anoxic conditions for the different performed experiments. Samples were then immediately frozen at −80 °C for preservation. DNA was extracted using the DNeasy PowerBiofilm Kit (Qiagen, Hilden, Germany). The concentration and purity of the extracted DNA were assessed using a NanoDrop 2000 spectrophotometer and a Qubit dsDNA assay Kit (Thermo Scientific, Waltham, MA, USA). DNA samples were stored at −20 °C until the MinION sequencing. Basecalling and demultiplexing were performed with dorado version 7.3.9 in super accuracy mode. Sequencing reads were aligned against metagenome-assembled genomes (MAGs) from the GTDN database [9] with BLAST v2.12 for taxonomic identification and abundance estimation. PCA was conducted, as a multivariate analysis tool, to study the combined impacts of different parameters on various performance indicators as well as microbial dynamics, using Minitab 22.3. Furthermore, co-occurrence network analysis based on Spearman correlations was conducted to highlight global interrelations among genera in response to all tested conditions, using R (version 4.1.0) and Gephi (version 0.10); only significant correlations ($p < 0.1$) were involved in the construction of the network.

3. Results and discussion

3.1. Effect of substrate concentration

MEC performance with hydrolysate concentrations of 20 %, 40 %, and 60 % was evaluated at pH 7 and anodic potential of 0 V vs SHE. These hydrolysate concentrations were selected to mimic potential dilution scenarios in full-scale plants, where primary sludge hydrolysate might be mixed with municipal wastewater or return streams, covering a range from low to high organic loading to systematically investigate the effect of substrate concentration. As shown in Fig. 2a, and consistent with current density profiles over time (see supplementary material), mean current density peaked at 40 % hydrolysate (i.e., 0.46 A/m^2; Fig. 2a), reflecting optimal substrate availability and microbial electron transfer capacity. Limited substrate and low conductivity (1.75 mS/cm) at 20 % hydrolysate reduced microbial activity and increased internal resistance, whereas at 60 %, high substrate concentration diverted electrons toward non-electrogenic pathways like methanogenesis, resulting in reduced current output relative to VFA degradation. Among the existing VFAs, acetate removal was most efficient, while butyrate removal remained limited. Although VFA and TOC removal rates kept increasing when increasing hydrolysate concentration, peaking at 60 % hydrolysate (i.e., 2.9, 2.2, and 32.6 mM/d for acetate, propionate, and TOC, respectively), TOC-based CE was highest at 40 % (i.e., 12.7 %; Fig. 2c), declining at lower (5.8 % at 20 % hydrolysate) and higher concentrations (2.7 % at 60 % hydrolysate; Fig. 2b). As expected, VFA-based CE was consistently higher than TOC-based CE across all

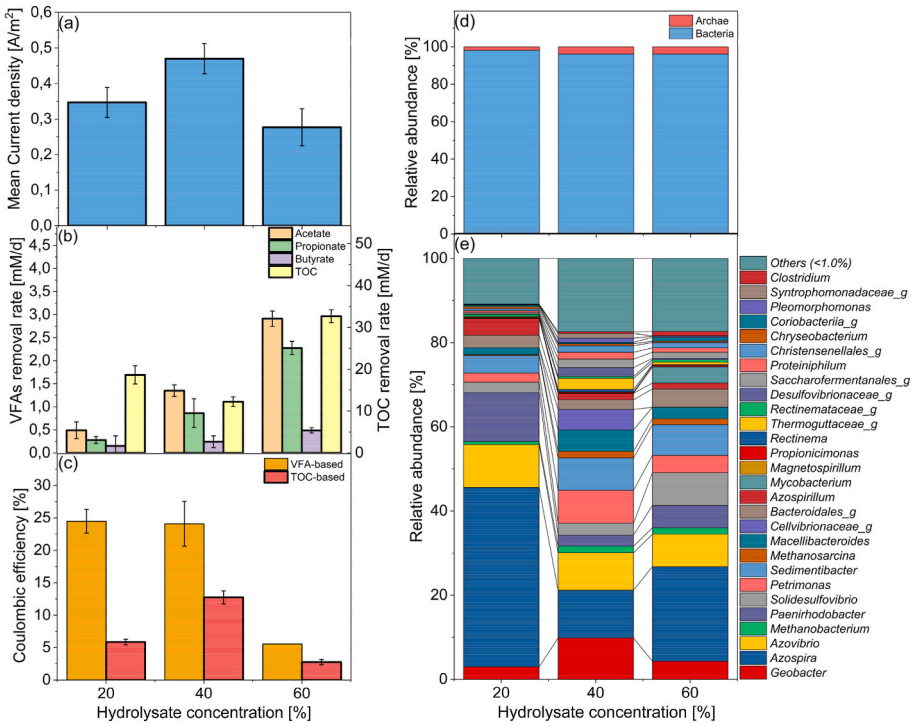

Fig. 2. Effects of hydrolysate concentration (20 %, 40 %, and 60 %) on microbial electrolysis cell performance. (a) Mean current density, (b) Volatile fatty acids (VFSs) and total organic carbon (TOC) removal rates, (c) Total organic carbon (TOC) and volatile fatty acid (VFA)-based coulombic efficiency (CE), (d) Microbial community composition at the domain level, and (e) Microbial community composition at the genus level.

conditions, with no significant difference between 20 % and 40 %, highlighting efficient VFA utilization but more favorable total electron recovery achieved at 40 % hydrolysate supporting previous findings on the importance of optimal substrate loading in BESs performance [33, 34].

By looking at the microbial composition of anodic biofilms, it was found that the domain-level composition remained stable across hydrolysate concentrations (Fig. 2d), with bacteria dominant and archaea comprising a minor fraction, increasing slightly from 1.9 % to 3.9 % when increasing hydrolysate concentration from 40 % to 60 %. When looking at the genus level classification, at 20 % hydrolysate, *Azospira* was the most abundant genus, known for its ability to utilize VFAs such as acetate as electron donors [23]; its high relative abundance may have partially contributed to the VFA consumption observed under these conditions (Fig. 2b), despite the limited current generation. The genus *Azospira*, known as a facultative anaerobic denitrifier [24], has been widely found in BESs; however, its direct involvement in extracellular electron transfer to anodes has yet to be confirmed [25,26]. Because the measure reflects relative abundance, this result likely stems from poor electroactive biofilm formation under these conditions, consistent with the low current density and CE observed. Aligning with this, the abundance of *Azospira* decreased at higher hydrolysate concentrations. A similar observation was reported by Li et al. [27], who showed that when COD increased from 200 to 400 mg/L, the relative abundance of *Azospira* decreased from 22.05 % to 9.77 %, suggesting that higher organic loading can reduce its competitiveness in BESs. The genus *Azospira* has been widely found in BESs; however, its direct involvement in extracellular electron transfer to anodes has yet to be confirmed [35, 36]. Additionally, the abundance of fermentative bacteria and *Geobacter* was relatively low, further limiting VFA production and electrogenic activity. At 40 % hydrolysate, a more optimal balance between fermentative bacteria, e.g., *Petrimonas*, *Macellibacteroides*, and *Proteiniphilum* [37–39], and exoelectrogens (e.g., *Geobacter*) might have facilitated effective VFA conversion and electron transfer to the anode, resulting in the highest current density and CE. At 60 % hydrolysate, *Azospira* and sulfate-reducing bacteria such as *Solidesulfovibrio* were enriched. Given their reported ability to utilize VFAs [40], they can potentially compete with exoelectrogens like *Geobacter* and divert electrons from current-generating pathways, contributing to reduced MEC performance.

Overall, the data emphasize that 40 %-hydrolysate provides the most favorable balance between substrate availability and microbial community function, supporting electron transfer and system performance.

3.2. *Effect of pH*

The effect of pH on MEC performance was evaluated across pH 5–8 using 40 % hydrolysate and an applied potential of 0 V. Mean Current density increased from 0.06 A/m^2 at pH 5 to 1.03 A/m^2 at pH 8 (Fig. 3a). Substrate degradation showed clear pH dependence (Fig. 3b). At pH 5–6.5, acetate and TOC removal were high, indicating effective carbon utilization, while propionate accumulation at pH 5–5.5 suggests reduced metabolic activity for its oxidation. At pH 6, peak removal efficiency was observed, with acetate, propionate, and butyrate consumed at 7.48, 2.70, and 1.36 mM/d, respectively, alongside TOC removal of 53.15 mM/d, suggesting that this range likely supports an optimal balance between fermentative activity and microbial community structure. Additionally, microbial biofilms can buffer local environments, creating microzones with near-neutral pH that support continued metabolic activity [41]. As shown in Fig. 3c–TOC-based CE was below 1 % at pH values below 6. However, CE increased sharply above this threshold, peaking at 18.6 % at pH 8. Low CE under acidic conditions likely resulted from electron diversion to non-electrogenic pathways and inhibition of electroactive microbes. As previously reported by Dhar et al. [42], *Geobacter*-dominated biofilms are sensitive to moderately acidic environments, with reduced activity or viability observed below pH 6.5. VFA-based CE showed no significant difference between pH 7 and 8, suggesting stable VFA conversion efficiency in this neutral to mildly alkaline range.

Domain-level microbial composition remained stable across pH 5, 7,

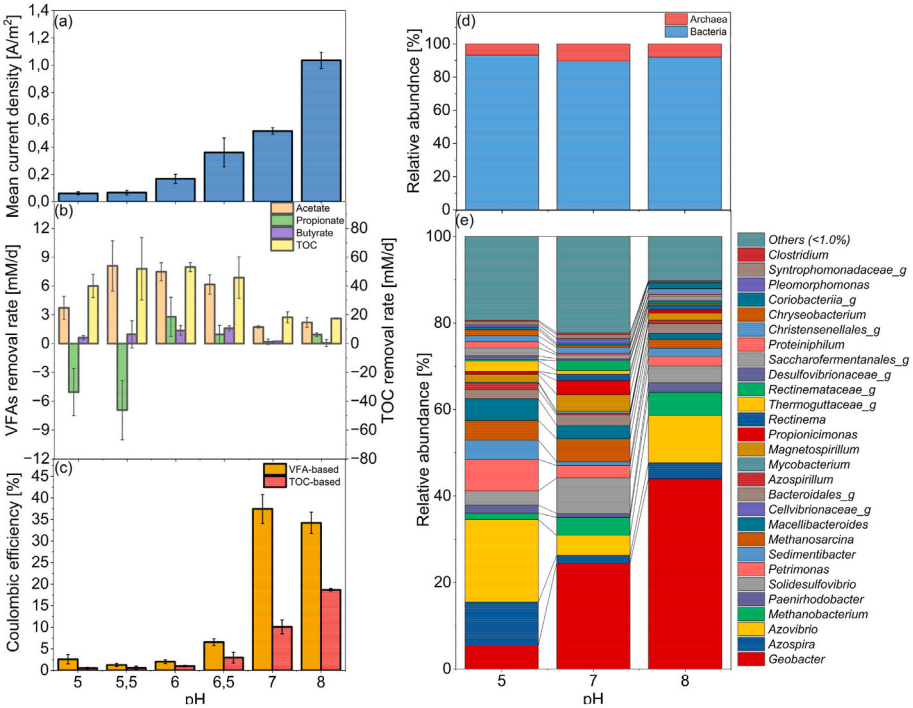

Fig. 3. Effects of pH on microbial electrolysis cell (MEC) performance. (a) Mean current density; (b) Volatile fatty acids (VFAs) and total organic carbon (TOC) removal rates, (c) Total organic carbon (TOC) and volatile fatty acid (VFA)-based coulombic efficiency (CE), (d) Microbial community composition at the domain level, and (e) Microbial community composition at the genus level.

and 8 (Fig. 3d), with bacteria consistently dominant (>90 %) and archaea representing a minor fraction. However, a slight but meaningful increase in archaeal abundance at pH 7 indicates that neutral conditions were more favorable for archaea. Slightly alkaline environments support the proliferation of electroactive bacteria such as *Geobacter* spp., which rely on direct anode respiration, while also suppressing non-electrogenic organisms. This microbial selection promotes more efficient substrate oxidation and electron capture [15,43], contributing to the observed increases in CE. At acidic pH (5–6), propionate accumulation could be due to the activity of the genus *Propionicimonas*. At these pH levels, the microbial community showed elevated abundances of fermentative bacteria (e.g., *Petrimonas*, *Sedimentibacter*, and *Macellibacteroides*) and methanogens such as *Methanosarcina*, while electroactive bacteria like *Geobacter* remained at low relative abundance. Notably, *Azospira* was more abundant under these acidic conditions. At neutral pH of 7, system performance improved, with higher mean current density and CE. The microbial community shifted toward electrogenic activity, characterized by an increase in *Geobacter* and a decrease in fermenters. At pH 8, performance peaked, with *Geobacter* dominating (i.e., 44 % relative abundance) and *Methanosarcina* significantly reduced. A bulk pH of 8 can buffer pH gradients and local acidification within the biofilm, due to the release of protons, which would otherwise inhibit key metabolic processes, disrupt proton transport, and reduce the efficiency of EET [44]. This stabilized microenvironment favors electroactive bacteria such as *Geobacter*. These findings agree with previous studies reporting that neutral-to-alkaline pH enhances electrogenic activity [43]. A reduction in methanogen abundance may be due to the reduced activity of key enzymes involved in both acetoclastic and hydrogenotrophic methanogenesis, as well as the inhibition of proteins essential for electron transport and ATP synthesis under alkaline conditions [45]. Methanogen suppression at high pH, due to their alkaline sensitivity, has been reported [17], allowing exoelectrogens to use available electrons for current generation better, leading to improved MEC performance.

The higher performance observed within the pH range of 7–8 can be attributed to the optimal activity of key enzymes involved in extracellular electron transfer (EET), such as multi-heme c-type cytochromes, within this pH range [44,46]. On the other hand, acidic conditions increase the redox potential and cause proton accumulation, which impairs electron flow and hinders EET activity, leading to lower efficiency [42]. These findings highlight the importance of pH control in supporting efficient current generation, sustained substrate degradation, and the development of a stable and functionally effective anodic microbial community. Although pH 8 resulted in the lowest organic acid removal, it produced the highest current density and is therefore suitable for systems in which hydrogen production is prioritized over organic pollutant removal. Therefore, in order to achieve higher overall organic-C removal, an optimized prior dark fermentation stage and/or a downstream treatment phase, which is usually the case when discharging the effluent to the sewage system, is required.

3.3. *Effect of applied anodic potential*

The effect of anodic potential on MEC performance was assessed at −0.2, 0, 0.2, and 0.4 V vs. SHE, using 40 % hydrolysate and pH 8. As shown in Fig. 4a, the mean current density was minimal at −0.2 V (0.08 A/m^2), increased to 0.88 A/m^2 at 0 V, and rose further to 2.44 A/m^2 and 3.40 A/m^2 at 0.2 V and 0.4 V, respectively, indicating enhanced electrochemical activity with increasing potential. This trend is attributed to the improved electrochemical driving force at more positive potentials, especially when dealing with complex substrates, which facilitates electron transfer from electroactive microorganisms to the electrode. As shown in Fig. 4b–TOC and acetate removal rates increased significantly with rising applied potential. TOC removal improved from 11.82 mM/d at −0.2 V to 30.24 mM/d at 0.4 V, while acetate removal increased from 0.67 to 3.92 mM/d across the same potential range, reflecting increased microbial oxidation and electron transfer efficiency. Propionate degradation peaked at 0–0.2 V but declined at 0.4 V, likely due to microbial shifts. Butyrate removal was minimal (<0.1 mM/d) across all voltages. These findings support previous studies that demonstrate higher voltages promote substrate degradation by increasing

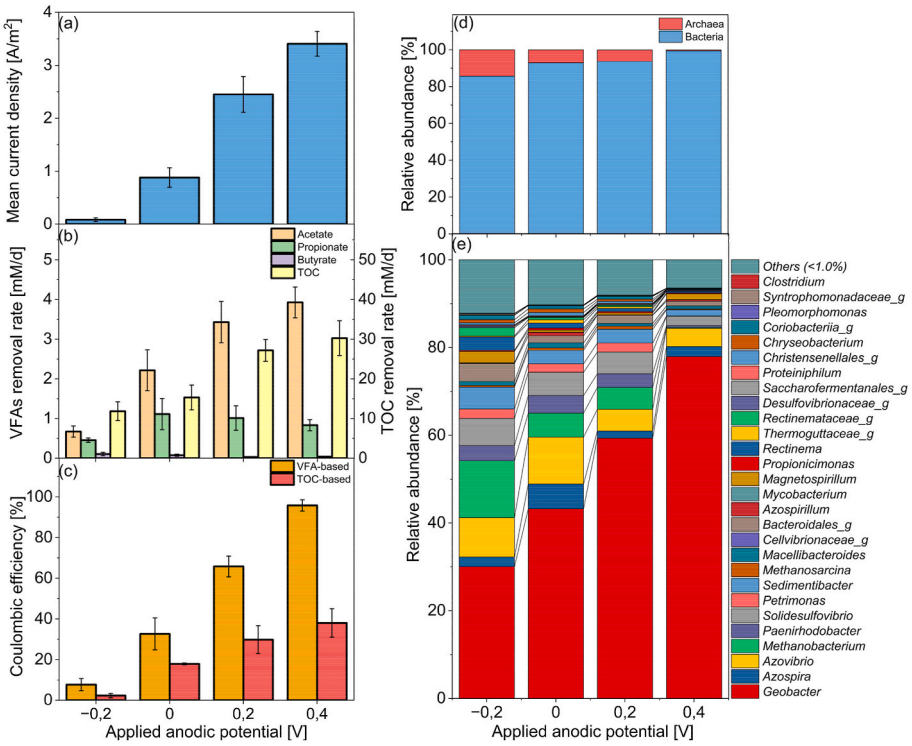

Fig. 4. Effect of applied anodic potential (−0.2 to 0.4 V vs. SHE) on microbial electrolysis cell performance. (a) Mean current density, (b) VFAs (acetate, propionate, butyrate) and total organic carbon removal rates, (c) Total organic carbon (TOC) and volatile fatty acid (VFA)-based coulombic efficiency (CE), (d) Microbial community composition at the domain level, and (e) Microbial community composition at the genus level.

electrochemical gradients and microbial activity [23,47]. TOC-based CE increased progressively with applied anodic potential, rising from 2.2 % at −0.2 V to 38.0 % at +0.4 V (Fig. 4c). VFA-based CE also showed a sharp increase, from 7.6 % at −0.2 V to 95.7 % at +0.4 V, approaching nearly complete recovery of electrons from VFAs. This upward trend indicates improved electron capture and transfer efficiency under more favorable redox conditions. Increasing potential improved substrate oxidation and electron flow, boosting exoelectrogen activity. The highest CE at 0.4 V indicates optimal microbial metabolism and efficient EET. In addition, the near-100 % VFA-based CE can be attributed to potential unconsidered intermediate acids production due to fermentation and/or minor internal hydrogen recirculation as an electron donor by *Geobacter*.

Domain-level microbial composition shifted with increasing anodic potential (Fig. 4d), with bacteria remaining the dominant group. At the same time, archaeal abundance declined from −0.2 V to 0.4 V, suggesting that higher potential created conditions unfavorable for archaea, especially methanogens, due to increased electrochemical activity or altered redox conditions. Meanwhile, the weak performance of MEC at an applied potential of −0.2 V correlated with a high relative abundance of hydrogenotrophic methanogens, such as *Methanobacterium*, which likely diverted electrons toward methane production rather than anodic reduction. Fermentative genera such as *Sedimentibacter* (4.99 %) and *Bacteroidales_g* (4.13 %) were prominent, indicating roles in hydrolysis and acidogenesis, although they do not contribute to electron transfer. At low potential, low *Geobacter* abundance limited the electron flow toward the anode. As potential increased, MEC performance improved with higher current density, CE, and VFA removal, driven by a shift toward exoelectrogens and a decrease in methanogens. At 0.4 V, performance peaked, with *Geobacter* dominating and methanogens and SRBs (like *Solidesulfovibrio)* declining, indicating that higher potential promotes exoelectrogens over competing microorganisms.

3.4. *Multivariate assessment of operational and microbial interactions*

To generalize the interactions among the tested parameters and resulting performance indicators as well as anodic microbial dynamics, PCA was conducted. Firstly, the analyzed interactions among the tested conditions and performance indicators are shown in Fig. 5a and b. The first two principal components (PC1 and PC2) accounted for 75.2 % of the total variance, indicating strong explanatory power and data interpretability. The score plot in Fig. 5a shows that employing acidic pH values (<7.0) induced noticeable variations with other conditions. Changing the anodic potential from −0.2 to +0.4 V vs SHE substantially contributed to the overall variations among samples. Further, the loading plot in Fig. 5b highlights the superior contribution of pH and anodic potential in the resulting variations among samples, as compared with hydrolysate concentration. Strong positive correlations between mean current density and both CE and anodic potential were observed, highlighting that organic carbon was the primary electron donor in the system, rather than an unfavorable contribution from cathodic hydrogen. However, this was not the case for acetate, butyrate, and TOC removal rates, which showed weak correlations with current density and CE. This suggests the presence of competing carbon-consumption pathways, including methanogenesis. Additionally, their strong positive correlations with hydrolysate concentration support this hypothesis.

Secondly, the interactions among the tested parameters and corresponding anodic microbial composition are shown in Fig. 5c and d, with a similarly high total variance of 68.3 % explained by PC1 and PC2. Slightly different from variations among performance indicators, it can be noticed that the anodic potential and hydrolysate concentration contribute equally (and lower than the pH contribution) to the obtained variations. The lowered contribution of anodic potential in total variance could be justified by its particular and very strong positive correlation with *Geobacter* (Fig. 5d). The figure clearly shows a strong positive correlation between *Geobacter* and both anodic potential and pH;

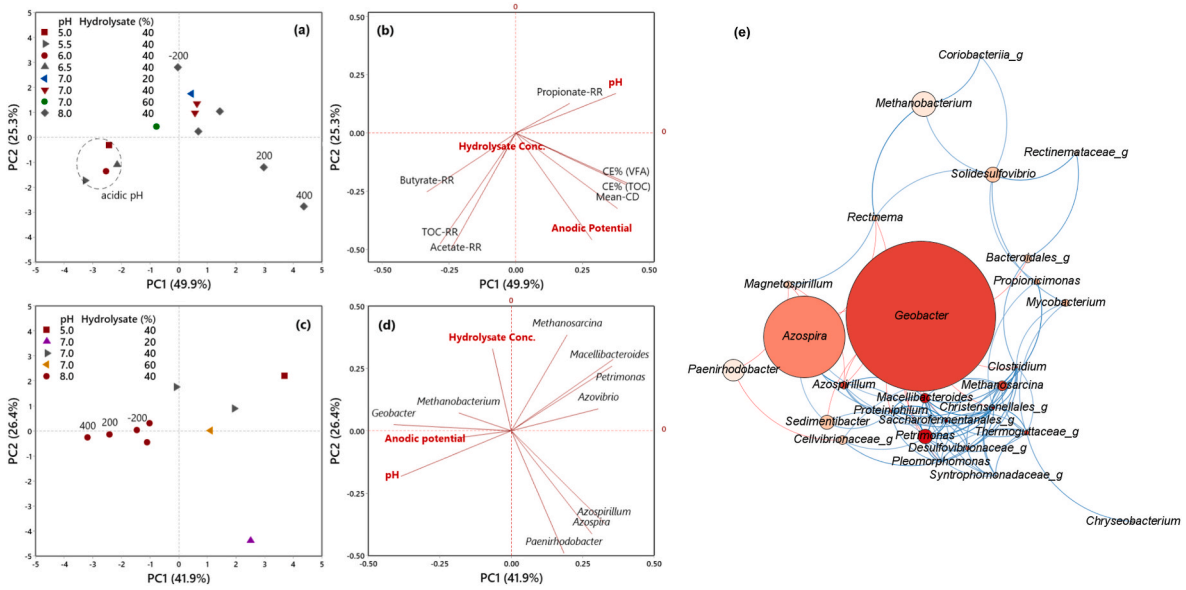

Fig. 5. Score and loading plots derived by PCA based on tested parameters, i.e., hydrolysate concentration (%), pH, and anodic potential (presented in mV and equals to 0 vs SHE unless otherwise mentioned), and the resulting MEC-performance indicators (a, b) or the resulting relative abundance of major genera identified in the anodic community (c, d). (e) Spearman correlation network showing microbial interactions within the anodic community under the tested conditions; only significant correlations ($p < 0.1$) are displayed; node size represents the maximum relative abundance of each genus across all samples; blue and red edges indicate positive and negative correlations, respectively; node color reflects the closeness centrality rank, with red indicating the highest and white the lowest. (For interpretation of the references to color in this figure legend, the reader is referred to the Web version of this article.)

however, strong negative correlations were observed between *Geobacter* and other microorganisms, particularly *Methanosarcina*. This observation aligns with the fact that the composition represents only the anodic community, where the dominance of exoelectrogenic bacteria, specifically *Geobacter* in this case, is expected to contribute most significantly to MEC efficiency. The observed positive correlation between *Geobacter* and the hydrogenotrophic methanogen *Methanobacterium* likely supports the potential (but minor) establishment of direct interspecies electron transfer (DIET) between both genera. The capability of *Methanobacterium* to perform DIET with *Geobacter* has been confirmed in earlier studies [48]. Given that this cooperation may compete with the anode for electrons, our hypothesis of considering this competition minor is supported by the corresponding increase in current density and CE.

Furthermore, to explore microbial interactions across all tested conditions, a co-occurrence network was constructed based on spearman correlations, visualizing only significant correlations among genera with relative abundances above 1 % (Fig. 5e). Given that the size of nodes represents the maximum obtained abundance of each genus in all samples, it can be clearly shown how *Geobacter*, followed by *Azospira*, developed across the tested conditions. As indicated by the network edges, *Geobacter* exhibited mostly negative correlations with other genera (e.g., *Azospira*, *Clostridium*, *Petrimonas*, and *Azospirillum*), highlighting its dominant and functionally critical role within the anodic consortium. In particular, the negative correlation between *Geobacter* and the abundant *Azospira* suggests that Azospira may have been a major competitor for carbon sources in the process. The genus *Azospira*, known to oxidize organic acids such as acetate, propionate, butyrate, and lactate, has previously been found abundant in BESs treating complex wastewater [35,49,50]. The numerous positive correlations among microbial genera—excluding *Geobacter*—such as *Clostridium*, *Methanosarcina*, *Petrimonas*, *Sedimentibacter*, *Desulfovibrionaceae*, and *Syntrophomonadaceae*, which are widely associated with anaerobic fermentation and subsequent methanogenesis [51], highlight their competing role within the anodic biofilm. Analysis of closeness centrality in the constructed network shows that both *Geobacter* and these major competitors are highly connected to other genera, emphasizing their counteractive interactions under the tested conditions.

3.5. Upscaling in a 10 L-RDBER: techno-economic assessment

To evaluate the influence of applied potential on system performance during scale-up, RDBER was operated under two different applied anodic potentials. The selected range was based on the C-MEC results and to emphasize the energy-efficiency considerations. The potential of 0 V vs SHE was considered as a practical lower bound providing sufficient overpotential for acetate oxidation, while +0.4 V vs SHE was examined as the potential to induce the highest current density, to eventually evaluate the energy efficiency of both potentials. The experiment started with synthetic medium, and following a 7-day enrichment phase using *G. sulfurreducens*, the medium was replaced with 40 % hydrolysate at pH 8. An anodic potential of 0 V was applied for 7 days, during which current density gradually increased, reaching to maximum 1.12 A/m^2 (Fig. 6a). This was accompanied by a steady decline in acetate and TOC concentrations, indicating active substrate oxidation (Fig. 6b). Following the depletion of acetate, a new batch cycle with 40 % hydrolysate was employed at higher anodic potential of +0.4 V. Under these conditions, a higher current density was achieved, peaking at 1.94 A/m^2. Acetate and TOC were consumed more rapidly compared to the 0 V phase, suggesting enhanced electron transfer and microbial metabolic activity at the elevated potential. Gas composition data (Fig. 6c) revealed that hydrogen was the dominant gas produced under both conditions, while methane (CH_4) remained consistently low throughout the experiment. The extremely low CH_4 concentrations, even after the system was fed with unsterile hydrolysate, highlight the scalability of the optimal operational conditions, i.e., pH and anodic potential, obtained by the 250 mL C-MECs. This also confirms the lower thermodynamic favorability of methanogenesis at optimized anodic biofilm conditions.

A comparative evaluation of hydrogen production rates from other studies using single-chamber MECs fed with real wastewater highlights the need to optimize both operational parameters and reactor configuration based on the substrate composition. For instance, in a pilot-scale continuous-flow MEC, Cusick et al. [52] achieved 6.08 L-H_2/m^2·d while

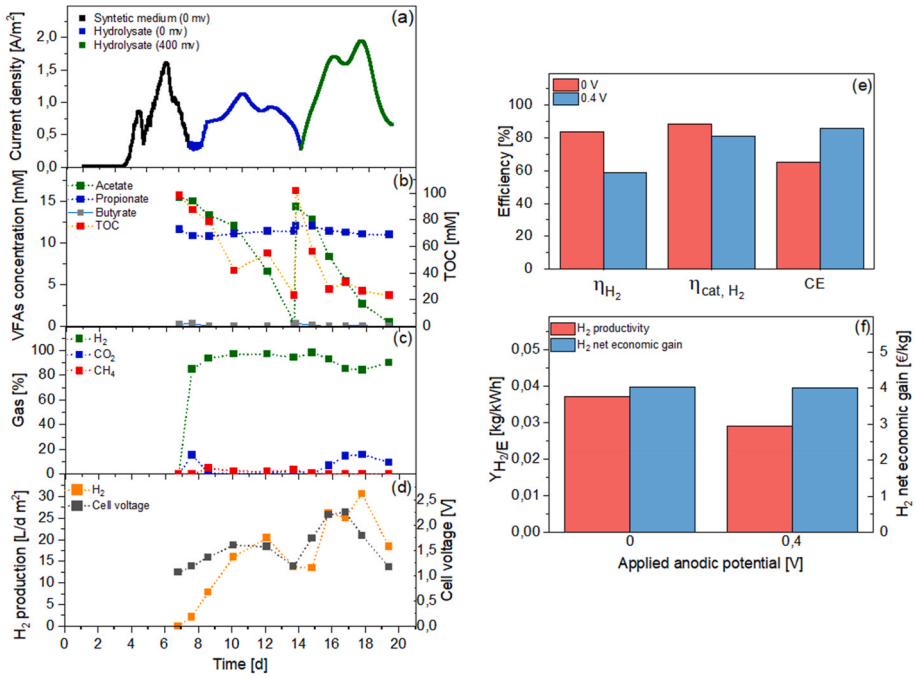

Fig. 6. Effect of applied anodic potential on the performance of a 10 L rotating disk bioelectrochemical reactor (RDBER). (a) Current density under two applied potentials: 0 V vs. SHE with synthetic medium (black) and hydrolysate (blue), and 0.4 V vs. SHE with hydrolysate (green), (b) Acetate and total organic carbon (TOC) concentrations, (c) Gas composition (% H_2, CO_2, CH_4), (d) hydrogen production rate and cell voltage over time, (e) hydrogen energy efficiency (η_{H2}), cathodic hydrogen recovery ($\eta_{cat,H2}$) and TOC-based Coulombic efficiency (CE), and (f) hydrogen yield per unit of energy input (kg H_2/kWh) and net economic gain (€/kg H_2). (For interpretation of the references to color in this figure legend, the reader is referred to the Web version of this article.)

treating winery wastewater, 0.9 V applied cell voltage and pH ≥ 6. Wang et al. [53] achieved 29.6 L-H_2/m^2·d in a 10 L batch-operated system treating lignocellulosic hydrolysate at 1.36 V applied cell voltage, with an energy efficiency of 62 %; Heidrich et al. [54] achieved 0.006 L-H_2/L d in a 88 L-MEC treating domestic wastewater at a cell voltage of 1.1 V, with an average energy efficiency of 48.7 % and CE of 41.2 %. Fan et al. [55] reported 0.32 L-H_2/m^2·d and 33 % CE in a 100 L-RDBER operated using synthetic medium at 0 V; in this study, however, the achieved maximum hydrogen production rate, CE, and energy efficiency were 30.57 L-H_2/m^2·d, 86.1 %, and 59 %, respectively, at applied anodic potential of +0.4 V.

Furthermore, to assess the energy efficiency of RDBER while producing H_2 from hydrolysate, the electrochemical, energetic, and economic performance were considered, in relation to the applied anodic potential. As shown in Fig. 6d, applying 0.4 V anodic potential increased the maximum cell voltage from 1.57 V (at 0 V) to 2.25 V. This trend paralleled hydrogen productivity, with peak voltages aligning with the maximum hydrogen gas evolution. The higher cell voltage indicates increased energy input, which impacts system efficiency and applicability. Hydrogen production was significantly higher under 0.4 V, reaching 30.57 L-H_2/m^2·d (based on cathode surface area), compared with the production at 0 V (i.e., 20.37 L-H_2/m^2·d). Despite this improvement in volumetric output, key energy efficiency metrics revealed that enhanced hydrogen yield does not necessarily correspond to more efficient energy utilization (Fig. 6e). Specifically, hydrogen energy efficiency (η_{H2}), defined as the ratio of the energy content of the produced hydrogen to the total electrical energy input, was higher at 0 V, reaching 83.7 %, compared to 59 % at 0.4 V. This indicates that, although hydrogen production was lower under lower applied potential, the system was more energy efficient. In contrast, the additional energy input at 0.4 V led to lower η_{H2} values, suggesting that the system was less efficient in recovering the supplied electrical energy into chemical energy in the form of hydrogen. Cathodic hydrogen recovery ($\eta_{cat,H2}$), was slightly lower at 0.4 V (81.0 %) compared to 88.5 % at 0 V. Although this indicates a modest reduction in the fraction of electrons converted to hydrogen, the difference is not substantial. The slight decrease at 0.4 V is likely attributed to increased utilization of the produced H_2 as an electron donor and/or to alternative cathodic pathways that do not contribute to hydrogen generation, such as sulfate or nitrate reduction, given their minor presence in the hydrolysate.

In contrast to η_{H2} and $\eta_{cat,H2}$, CE increased with the applied anodic potential, indicating improved electron recovery from substrate oxidation as measured by the current. This trend is likely associated with enhanced activity of electroactive bacteria and more favorable conditions for EET at elevated potentials. The increased CE suggests that a greater proportion of the chemical energy from the substrate was captured electrochemically; however, the observed discrepancy between CE and the other efficiency metrics indicates that not all electrons contributing to current ultimately ended up in hydrogen production. Fig. 6f further supports these observations. Hydrogen yield normalized to energy input was higher at 0 V (0.03 kg H_2/kWh) compared to 0.4 V (0.02 kg H_2/kWh), highlighting the superior energy conversion efficiency at 0 V. Notably, the net economic gain remained similar across both operating conditions, 4.02 and 4.01 €/kg H_2 at 0 V and 0.4 V, respectively, indicating that although energy efficiency was lower at 0.4 V, the increased hydrogen production helped offset the additional energy cost from an economic perspective. Overall, these findings demonstrate that while the application of anodic potential enhances hydrogen production and electron recovery, it adversely affects hydrogen energy efficiency. Therefore, system operation at 0 V is likely preferable when maximizing energy efficiency is the primary objective, whereas operation at 0.4 V is justified in applications prioritizing volumetric productivity or capacity.

Overall, for continuous operation of membraneless-MECs fed with hydrolysate, maintaining the pH at 8 and applying anodic potential of +0.4 V are recommended to support stable electroactive biofilms and suppress competing pathways. In addition, due to the high organic strength of hydrolysate, adequate dilution is recommended to maintain the effective loading rate. This can be achieved either through a defined effluent-to-influent recirculation ratio or by adjusting the hydraulic

retention time, thereby improving operational stability and hydrogen recovery.

4. Conclusions

Substrate-based tuning was found to be crucial for optimizing MEC efficiency. Sludge-hydrolysate concentration above 40 % reduced MEC performance, due to increased competition for carbon with exoelectrogens, indicating that moderate organic loading is more effective. Alkaline pH enhanced MEC efficiency by shifting the microbial composition toward more efficient exoelectrogenesis, likely by regulating the H^+-gradient within anodic biofilm. Higher anodic potentials further increased electrochemical efficiency by facilitating EET, allowing *Geobacter* to outcompete other microorganisms. Optimal performance was achieved at 40 %-hydrolysate, pH 8, and +0.4 V, yielding a current density of 3.4 A/m^2, while enriching *Geobacter* and minimizing methanogenic activity. In the scaled-up system, hydrogen production peaked at +0.4 V (30.57 L/m^2/d), but energy efficiency was higher at 0 V (83.7 % vs. 59 %). Nonetheless, net economic returns remained comparable (~4 €/kg H_2), supporting the feasibility of productivity-focused operation. These results demonstrate that coordinated optimization of biological and electrochemical parameters is key to advancing MECs toward practical energy recovery applications.

CRediT authorship contribution statement

Mahshid Golalikhani: Writing – original draft, Visualization, Validation, Methodology, Investigation, Formal analysis, Data curation, Conceptualization. **Christian Jonas Lapp:** Validation, Investigation, Formal analysis, Data curation. **Nikhil Shylaja Prakash:** Resources, Investigation, Formal analysis. **Andrea Hille-Reichel:** Writing – review & editing, Resources. **Johannes Gescher:** Writing – review & editing, Supervision, Resources, Project administration, Methodology, Investigation, Funding acquisition, Conceptualization. **Ahmed Elreedy:** Writing – review & editing, Writing – original draft, Validation, Methodology, Investigation, Formal analysis, Conceptualization.

Declaration of generative AI and AI-assisted technologies in the writing process

During the preparation of this work the authors used ChatGPT-4 (OpenAI) to improve the readability and language of this manuscript. After using this tool, the authors reviewed and edited the content as needed, and take full responsibility for the content of the published article.

Declaration of competing interest

The authors declare that they have no known competing financial interests or personal relationships that could have appeared to influence the work reported in this paper.

Acknowledgment

This work was financially supported by the Baden-Württemberg Ministry for the Environment, Climate and Energy Management and the European Union (EU) within the framework of the European Regional Development Fund (ERDF) for the project KoalAplan (grant number: Bioök_2076413). The authors would like to thank research assistants Nadine Wagner and Johannes Carstensen for their support in carrying out the experiments.

Appendix A. Supplementary data

Supplementary data to this article can be found online at https://doi.org/10.1016/j.ijhydene.2025.153107.

Data availability

The data that has been used is confidential.

References

[1] Shen R, Liu Z, He Y, Zhang Y, Lu J, Zhu Z, et al. Microbial electrolysis cell to treat hydrothermal liquefied wastewater from cornstalk and recover hydrogen: degradation of organic compounds and characterization of microbial community. Int J Hydrogen Energy 2016;41:4132–42. https://doi.org/10.1016/j.ijhydene.2016.01.032.

[2] Yun WH, Yoon YS, Yoon HH, Nguyen PKT, Hur J. Hydrogen production from macroalgae by simultaneous dark fermentation and microbial electrolysis cell with surface-modified stainless steel mesh cathode. Int J Hydrogen Energy 2021. https://doi.org/10.1016/j.ijhydene.2021.09.168.

[3] Lalaurette E, Thammannagowda S, Mohagheghi A, Maness PC, Logan BE. Hydrogen production from cellulose in a two-stage process combining fermentation and electro hydrogenesis. Int J Hydrogen Energy 2009;34:6201–10. https://doi.org/10.1016/j.ijhydene.2009.05.112.

[4] Wang A, Liu W, Cheng S, Xing D, Zhou J, Logan BE. Source of methane and methods to control its formation in single chamber microbial electrolysis cells. Int J Hydrogen Energy 2009;34:3653–8. https://doi.org/10.1016/j.ijhydene.2009.03.005.

[5] Cusick RD, Kiely PD, Logan BE. A monetary comparison of energy recovered from microbial fuel cells and microbial electrolysis cells fed winery or domestic wastewaters. Int J Hydrogen Energy 2010;35:8855–61. https://doi.org/10.1016/j.ijhydene.2010.06.077.

[6] Hu H, Fan Y, Liu H. Hydrogen production in single-chamber tubular microbial electrolysis cells using non-precious-metal catalysts. Int J Hydrogen Energy 2009;34:8535–42. https://doi.org/10.1016/j.ijhydene.2009.08.011.

[7] Ali M, Elreedy A, Fujii M. Impacts of micro-to nano-sized carbon supplements on mixed and archaea-free halophilic cultures when used for bioenergy recovery from saline wastewater. J Clean Prod 2024;447:141478. https://doi.org/10.1016/j.jclepro.2024.141478.

[8] Asrul MAM, Atan MF, Yun HAH, Wahab NA, Hung HH, Lai JCH, et al. Optimization of mathematical modeling of microbial electrolysis cell for the production of hydrogen from sago wastewater substrate. ASEAN Eng J 2024;14:7–17. https://doi.org/10.11113/aej.V14.20419.

[9] Elreedy A, Härrer D, Ali R, Hille-Reichel A, Gescher J. Efficacious enrichment of butyrate-oxidizing exoelectrogens upgrades energy recovery in relevant bioelectrochemical systems. Environ Technol Innov 2024;36:103871. https://doi.org/10.1016/j.eti.2024.103871.

[10] Lu L, Xing D, Liu B, Ren N. Enhanced hydrogen production from waste activated sludge by cascade utilization of organic matter in microbial electrolysis cells. Water Res 2012;46:1015–26. https://doi.org/10.1016/j.watres.2011.11.073.

[11] Lu L, Ren N, Zhao X, Wang H, Wu D, Xing D. Hydrogen production, methanogen inhibition and microbial community structures in psychrophilic single-chamber microbial electrolysis cells. Energy Environ Sci 2011;4:1329–36. https://doi.org/10.1039/c0ee00588f.

[12] Jadhav DA, Chendake AD, Schievano A, Pant D. Suppressing methanogens and enriching electrogens in bioelectrochemical systems. Bioresour Technol 2019;277:148–56. https://doi.org/10.1016/j.biortech.2018.12.098.

[13] Saini K, Kumar SS, Kumar V, Bajar S. Utilizing sulfate-reducing bacteria in bioelectrochemical systems for industrial wastewater treatment: a comprehensive review. Bioprocess Biosyst Eng 2025. https://doi.org/10.1007/s00449-025-03256-9.

[14] Jin X, Liu H. The role of denitrifying bacteria within the bioelectrochemical system for nitrate-containing wastewater treatment. Bioelectrochemical systems, vol. 2. Singapore: Springer; 2020. https://doi.org/10.1007/978-981-15-6868-8_11.

[15] Sun H, Li J, Yang M, Shao Q. Influence of initial pH on anodic biofilm formation in single-chambered microbial electrolysis cells. Pol J Environ Stud 2019;28:1377–84. https://doi.org/10.15244/pjoes/89503.

[16] Nam JY, Logan BE. Enhanced hydrogen generation using a saline catholyte in a two chamber microbial electrolysis cell. Int J Hydrogen Energy 2011;36:15105–10. https://doi.org/10.1016/j.ijhydene.2011.08.106.

[17] Cui W, Luo H, Liu G. Efficient hydrogen production in single-chamber microbial electrolysis cell with a fermentable substrate under hyperalkaline conditions. Waste Manag 2023;171:173–83. https://doi.org/10.1016/j.wasman.2023.08.017.

[18] Zou L, Zhao X, Wu K, Liang C, Liu J, Yang H, et al. Multi-objective optimization for microbial electrolysis cell-assisted anaerobic digestion of swine manure. Int J Hydrogen Energy 2024;77:545–56. https://doi.org/10.1016/j.ijhydene.2024.06.166.

[19] Joicy A, Seo H, Lee ME, Kim DH, Cho SK, Ahn Y. Enhanced methane production using pretreated sludge in MEC-AD system: performance, microbial activity, and implications at different applied voltages. Int J Hydrogen Energy 2022;47:40731–41. https://doi.org/10.1016/j.ijhydene.2022.07.154.

[20] Call D, Logan BE. Hydrogen production in a single chamber microbial electrolysis cell lacking a membrane. Environ Sci Technol 2008;42:3401–6. https://doi.org/10.1021/es8001822.

[21] Hari AR, Venkidusamy K, Katuri KP, Bagchi S, Saikaly PE. Temporal microbial community dynamics in microbial electrolysis cells - influence of acetate and propionate concentration. Front Microbiol 2017;8:1–14. https://doi.org/10.3389/fmicb.2017.01371.

[22] Nam JY, Logan BE. Optimization of catholyte concentration and anolyte pHs in two chamber microbial electrolysis cells. Int J Hydrogen Energy 2012;37:18622–8. https://doi.org/10.1016/j.ijhydene.2012.09.140.
[23] Lim SS, Fontmorin JM, Izadi P, Wan Daud WR, Scott K, Yu EH. Impact of applied cell voltage on the performance of a microbial electrolysis cell fully catalysed by microorganisms. Int J Hydrogen Energy 2020;45:2557–68. https://doi.org/10.1016/j.ijhydene.2019.11.142.
[24] Nam JY, Tokash JC, Logan BE. Comparison of microbial electrolysis cells operated with added voltage or by setting the anode potential. Int J Hydrogen Energy 2011;36:10550–6. https://doi.org/10.1016/j.ijhydene.2011.05.148.
[25] Härrer D, Elreedy A, Ali R, Hille-Reichel A, Gescher J. Probing the robustness of Geobacter sulfurreducens against fermentation hydrolysate for uses in bioelectrochemical systems. Bioresour Technol 2023;369:128363. https://doi.org/10.2139/ssrn.4239421.
[26] Shen R, Zhao L, Lu J, Watson J, Si B, Chen X, et al. Treatment of recalcitrant wastewater and hydrogen production via microbial electrolysis cells. Int J Agric Biol Eng 2019;12:179–89. https://doi.org/10.25165/j.ijabe.20191205.5061.
[27] Shylaja Prakash N, Maurer P, Horn H, Hille-Reichel A. Valorization of organic carbon in primary sludge via semi-continuous dark fermentation: first step to establish a wastewater biorefinery. Bioresour Technol 2024;397:130467. https://doi.org/10.1016/j.biortech.2024.130467.
[28] Klein E, Wurst R, Rehnlund D, Gescher J. Elucidating the development of cooperative anode-biofilm-structures. Biofilms 2024;7:100193. https://doi.org/10.1016/j.bioflm.2024.100193.
[29] Hackbarth M, Gescher J, Horn H, Reiner JE. A scalable, rotating disc bioelectrochemical reactor (RDBER) suitable for the cultivation of both cathodic and anodic biofilms. Bioresour Technol Rep 2023;21:101357. https://doi.org/10.1016/j.biteb.2023.101357.
[30] Knoll MT, Jürgensen N, Weiler JR, Gescher J. Predictability and robustness of anode biofilm to changing potential in microbial electrolysis system. Bioresour Technol Rep 2023;24:101640. https://doi.org/10.1016/j.biteb.2023.101640.
[31] Eurostat. Electricity price statistics. https://ec.europa.eu/eurostat/statistics-explained/index.php?title=Electricity_price_statistics; 2025.
[32] Mission Innovation Hydrogen Valley Platform. Hydrogen cost and sales prices. https://h2v.eu/analysis/statistics/financing/hydrogen-cost-and-sales-prices; 2025.
[33] Ullah Z, Zeshan S. Effect of substrate type and concentration on the performance of a double chamber microbial fuel cell. Water Sci Technol 2020;81:1336–44. https://doi.org/10.2166/wst.2019.387.
[34] Jalil Anam, Yu Z. Impact of substrates , volatile fatty acids , and microbial communities on biohydrogen production : a systematic review and meta-analysis. Sustainability 2024:1–23. https://doi.org/10.3390/su162310755.
[35] Xiao Y, Zheng Y, Wu S, Zhang EH, Chen Z, Liang P, et al. Pyrosequencing reveals a core community of anodic bacterial biofilms in bioelectrochemical systems from China. Front Microbiol 2015;6:1410. https://doi.org/10.3389/fmicb.2015.01410.
[36] Koch C, Harnisch F. Is there a specific ecological niche for electroactive microorganisms? Chemelectrochem 2016;3:1282–95. https://doi.org/10.1002/celc.201600079.
[37] Cardeña R, Cercado B, Buitrón G. Microbial electrolysis cell for biohydrogen production. Biomass, biofuels, biochem. Biohydrogen. second ed. Elsevier; 2019. p. 159–85. https://doi.org/10.1016/B978-0-444-64203-5.00007-1.
[38] Board TE. Petrimonas . Bergey's man syst Archaea bact, vol. 8; 2015. p. 1–2. https://doi.org/10.1002/9781118960608.gbm00245.
[39] Feng G, Zeng Y, Wang HZ, Chen YT, Tang YQ. Proteiniphilum and Methanothrix harundinacea became dominant acetate utilizers in a methanogenic reactor operated under strong ammonia stress. Front Microbiol 2023;13. https://doi.org/10.3389/fmicb.2022.1098814.
[40] Sun Y, ter Heijne A, Rijnaarts H, Chen WS. The effect of anode potential on electrogenesis, methanogenesis and sulfidogenesis in a simulated sewer condition. Water Res 2022;226:119229. https://doi.org/10.1016/j.watres.2022.119229.
[41] Tran P, Lander SM, Prindle A. Active pH regulation facilitates Bacillus subtilis biofilm development in a minimally buffered environment. mBio 2024;15. https://doi.org/10.1128/mbio.03387-23.
[42] Dhar BR, Sim J, Ryu H, Ren H, Santo Domingo JW, Chae J, et al. Microbial activity influences electrical conductivity of biofilm anode. Water Res 2017;127:230–8. https://doi.org/10.1016/j.watres.2017.10.028.
[43] Halim MA, Rahman MO, Ibrahim M, Kundu R, Biswas BK. Effect of anolyte pH on the performance of a dual-chambered microbial fuel cell operated with different biomass feed. J Chem 2021;2021. https://doi.org/10.1155/2021/5465680.
[44] Bond DR, Strycharz-glaven SM, Tender LM, Torres CI. On electron transport through geobacter biofilms. https://doi.org/10.1002/cssc.201100748; 2012.
[45] Qiu S, Zhang X, Xia W, Li Z, Wang L, Chen Z, et al. Effect of extreme pH conditions on methanogenesis: methanogen metabolism and community structure. Sci Total Environ 2023;877:162702. https://doi.org/10.1016/j.scitotenv.2023.162702.
[46] Teixeira LR, Cordas CM, Fonseca MP, Duke NEC. Modulation of the redox potential and electron/proton transfer mechanisms in the outer membrane cytochrome OmcF from Geobacter sulfurreducens, vol. 10; 2020. p. 1–12. https://doi.org/10.3389/fmicb.2019.02941.
[47] Yan X, Peng P, Li X, Miao Y, Chen L, Zhao F. Bridging energy and microbes: how the anodic potential of microbial electrolysis cell improves anaerobic digestion. J Power Sources 2024;623:235489. https://doi.org/10.1016/j.jpowsour.2024.235489.
[48] Zheng S, Liu F, Wang B, Zhang Y, Lovley DR. Methanobacterium capable of direct interspecies electron transfer. Environ Sci Technol 2020;54:15347–54. https://doi.org/10.1021/acs.est.0c05525.
[49] Xin X, Qiu W. Linking microbial mechanism with bioelectricity production in sludge matrix-fed microbial fuel cells: freezing/thawing liquid versus fermentation liquor. Sci Total Environ 2021;752:141907. https://doi.org/10.1016/j.scitotenv.2020.141907.
[50] Achenbach LA, Michaelidou U, Bruce RA, Fryman J, Coates JD. Dechloromonas agitata gen nov, sp nov and Dechlorosoma suillum gen. nov., sp. Nov., two novel environmentally dominant (per)chlorate-reducing bacteria and their phylogenetic position. Int J Syst Evol Microbiol 2001;51:527–33. https://doi.org/10.1099/00207713-51-2-527.
[51] Yi Y, Wang HZ, Chen YT, Gou M, Xia ZY, Hu B, et al. Identification of novel Butyrate- and acetate-oxidizing bacteria in butyrate-fed mesophilic anaerobic chemostats by DNA-based stable isotope probing. Microb Ecol 2019. https://doi.org/10.1007/s00248-019-01400-z.
[52] Cusick RD, Bryan B, Parker DS, Merrill MD, Mehanna M, Kiely PD, et al. Performance of a pilot-scale continuous flow microbial electrolysis cell fed winery wastewater. Appl Microbiol Biotechnol 2011;89:2053–63. https://doi.org/10.1007/s00253-011-3130-9.
[53] Wang L, Long F, Liang D, Xiao X, Liu H. Hydrogen production from lignocellulosic hydrolysate in an up-scaled microbial electrolysis cell with stacked bio-electrodes. Bioresour Technol 2021;320:124314. https://doi.org/10.1016/j.biortech.2020.124314.
[54] Heidrich ES, Edwards SR, Dolfing J, Cotterill SE, Curtis TP. Performance of a pilot scale microbial electrolysis cell fed on domestic wastewater at ambient temperatures for a 12month period. Bioresour Technol 2014;173:87–95. https://doi.org/10.1016/j.biortech.2014.09.083.
[55] Fan S, Wykes MSD, Lin WE, Jones RL, Robins AG, Linden PF. Evaluation of key operational parameters in a novel pilot-scale rotating disk bioelectrochemical reactor for hydrogen production in a wastewater biorefinery Nikhil. Build Environ 2025:107386. https://doi.org/10.1016/j.cej.2025.168691.